

Quasiperiodicity in decagonal phases forced by inclined net planes?

Walter Steurer* and Antonio Cervellino

Laboratory of Crystallography, ETHZ, CH-8006 Zurich, Switzerland. Correspondence e-mail: steurer@kristall.erdw.ethz.ch

It is generally assumed that decagonal quasicrystals show periodically arranged atomic layers only on net planes perpendicular to the tenfold axis and quasiperiodically arranged ones parallel to it. However, there also do exist only slightly puckered atomic layers that are periodically arranged *and* inclined to the tenfold axis. They coincide with the net planes of the periodic average structures of the decagonal phase and are related to the strongest Bragg reflections. Since they link quasiperiodic and periodic directions, inclined net planes may play a crucial role for growth and stabilization of decagonal quasicrystals. In fact, it is shown how ideal quasiperiodic long-range order and inflation symmetry allow for the existence of inclined net planes with *small* corrugation and reinforce the relation with the periodic average structures.

© 2001 International Union of Crystallography
Printed in Great Britain – all rights reserved

1. Introduction

Crystal structures can be resolved into sets of N infinite stacks of atomic layers on net planes (lattice planes) (hkl) with spacing d_{hkl} . Each infinite stack contains the translation set of one of the N atoms per unit cell. The atoms on a single net plane occupy the nodes of a two-dimensional (2D) sublattice of the crystal lattice. In many cases, the relation holds that the larger the spacing d_{hkl} between net planes of a stack the higher is the net plane's atomic density and the stronger are the related Bragg reflections hkl . In the common case that the strongest attractive interactions are between densely packed atoms, these net planes are of high morphological importance (Donnay & Harker, 1937). Strong Bragg reflections mark also those net planes that strongly reflect conduction electrons leading to the formation of pseudogaps in the electron density of states (see *e.g.* Ashcroft & Mermin, 1976).¹

For quasicrystals, the situation is somewhat different. Owing to the lack of periodicity and of a lattice, there cannot exist any lattice planes. However, stacks of net-plane-like 'dense' atomic layers have also been identified in quasicrystals such as icosahedral Al–Mn–Pd (Boudard *et al.*, 1992), for instance. The spacings between these layers, however, follow quasiperiodic sequences. Thus, the sets of symmetrically equivalent stacks of net planes (for quasicrystals the term

'lattice plane' seems to be inadequate) form 3D quasiperiodic hexagrids (*cf.* Levine & Steinhardt, 1986; Socolar & Steinhardt, 1986). The morphology of icosahedral quasicrystals, point group $m\bar{3}5$, is characterized by special crystal forms with low Miller indices such as the pentagon-dodecahedron (01 τ) or the rhomb-triacacontahedron (111) (*cf.* Jaszczak, 1994, and references therein).

What is the situation in the case of decagonal quasicrystals (DQC)? The structure of DQC can be described geometrically (not crystal-chemically!) as periodic stackings of quasiperiodic atomic layers (*cf.* Steurer & Haibach, 1999a, and references therein). Thus, one obvious set of net planes is formed just by the stack of quasiperiodic layers itself. These may be regarded as 'lattice planes' in a proper sense. Additionally, five symmetrically equivalent stacks of net planes perpendicular to the quasiperiodic plane can easily be identified. The traces of such net planes may correspond to the Ammann lines in a Penrose tiling (Levine & Steinhardt, 1986; Socolar & Steinhardt, 1986), for instance. Ammann lines have the property that they cut the two unit tiles in the Penrose tiling always in the same way as lattice planes do with the unit cell of periodic crystals. The interplanar spacings follow a quasiperiodic sequence. The well known decaprismatic equilibrium morphology of DQC, point group $10/m\bar{m}m$, reflects the morphological importance of these net planes. In summary, DQC show sets of net planes orthogonal to the periodic axis with periodic spacing and other sets orthogonal to the quasiperiodic plane with quasiperiodic spacing. Owing to this strong characterization, each of these sets of net planes contains exactly all the atoms in the quasicrystal. Hence the electron density and the atomic packing density on such planes is in inverse ratio with their interplanar spacing.

¹ It is still not completely clear to which degree the Bloch-wave picture can be applied to electrons in a quasiperiodic potential, but there are good indications in this direction (Huang & Gong, 1998). This is probably the foremost issue for the comparison between periodic and aperiodic long-range order because it will clarify to what extent inflation symmetry can substitute periodic translation symmetry and allow for extended electron states.

The simple decaprismatic equilibrium habitus of DQC is well known. However, the growth morphology visible on tiny needle-like crystals of DQC is characterized by many facets inclined to the tenfold axis additionally to the common decaprism faces (Fig. 1). These facets correspond to planes relating periodic and quasiperiodic directions and indicate the existence of dense atomic layers in DQC on net planes *inclined* to the tenfold axis. Evidently, they are stable substructures, stable enough to be morphologically important. Their analysis is not straightforward because planes cutting the tenfold axis periodically cannot cut the quasiperiodic plane quasiperiodically at the same time and *vice versa*. Hence, it is impossible to have all the atoms *exactly* on a set of planes. We will however show how, allowing for a small amount of corrugation, this condition may be achieved.

The following discussion is based on the concept of ‘periodic average structure of quasicrystals’ (Steurer, 1999; Steurer & Haibach, 1999b; Steurer, 2001). The results allow us to determine the correlation between quasiperiodic and periodic directions in DQC. This in turn is useful to interpret the height distribution of terraces in surface studies, to find diffusion paths, to understand the growth morphology, glide systems and crack propagation in deformation experiments and, last but not least, to have a further insight on the stability of DQC. In fact, currently the structural stability investigation has been mostly confined within the quasiperiodic planes with little or no investigation of their relation to the 3D crystal to which they physically belong.

2. Discussion

2.1. Where are the net planes?

The prototype DQC on which our analysis is based is the basic decagonal phase $\text{Al}_{71}\text{Co}_7\text{Ni}_{22}$. For an introduction into the crystallography of quasicrystals, see, for instance, Steurer & Haibach (1999a). This phase is characterized (Cervellino *et al.*, 2001) by the quasilattice parameters $a = 3.757$, $c \equiv a_5 = 4.0855 \text{ \AA}$; there are two inversion-related quasiperiodic layers per c period, space group $P10_5/mmc$. $a_r = 2\tau a/5 = 2.432 \text{ \AA}$ is the edge length of a Penrose unit tile whose vertices cover all atomic sites and also the minimal nearest-neighbour atomic distance; $\tau = 2 \cos \pi/5 = (1 + 5^{1/2})/2 = 1.618 \dots$ is the golden mean. The parameters a and c are just the inverse of the lengths (*i.e.* the physical space projection lengths) of the reciprocal-space vectors (10000) and (00001), respectively.

The existence of net planes in a DQC can best be checked on the two characteristic 2D structure projections upon the (x_1, x_3) and the (x_2, x_3) planes (Fig. 2; x_1, x_2, x_3 are parallel- and x_4, x_5 are perpendicular-space Cartesian coordinates, x_3 is along the periodic axis with period c). Looking under grazing incidence, it is possible to notice other planes besides the obvious ones parallel or perpendicular to the tenfold axis. The (01101) and the $(\bar{1}\bar{1}112)$ inclined net planes, for instance, are easily identified. These planes are perpendicular to the reciprocal-space vectors $\mathbf{H}_1 = (01101)$ and $\mathbf{H}_2 = (\bar{1}\bar{1}112)$,

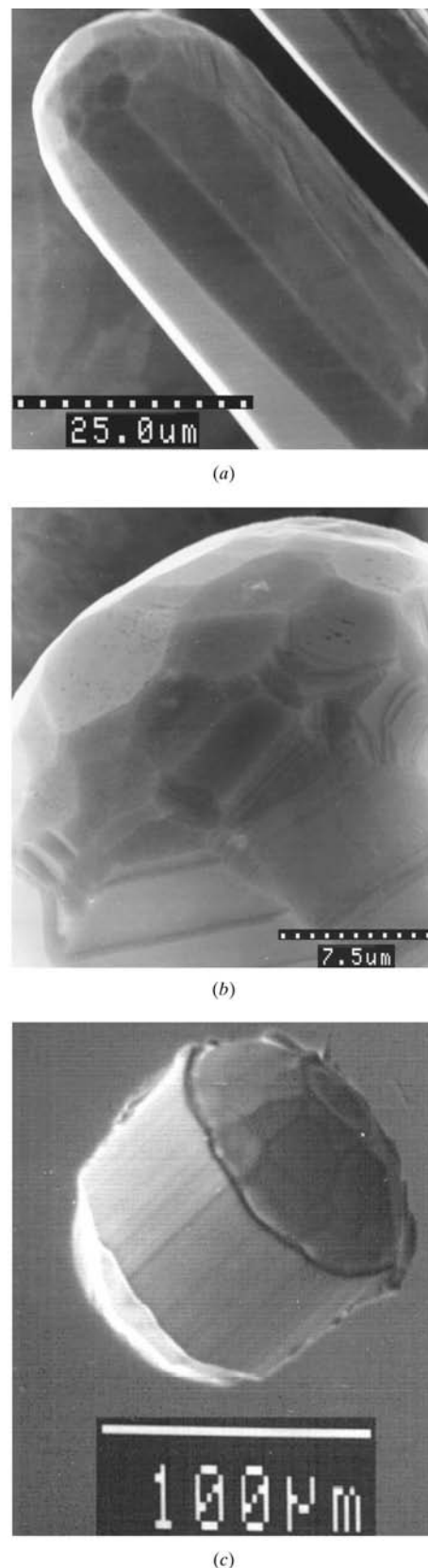


Figure 1 (a), (b) Growth morphology of tiny decaprismatic needles of decagonal Al–Co–Ni (courtesy of A. P. Tsai). (c) Facetted pore in decagonal Al–Co–Cu (courtesy of B. Grushko). The needles and the pore show beside the decaprism faces $\{100\bar{1}0\}$ many facets inclined to the tenfold axis (*i.e.* the needle axis).

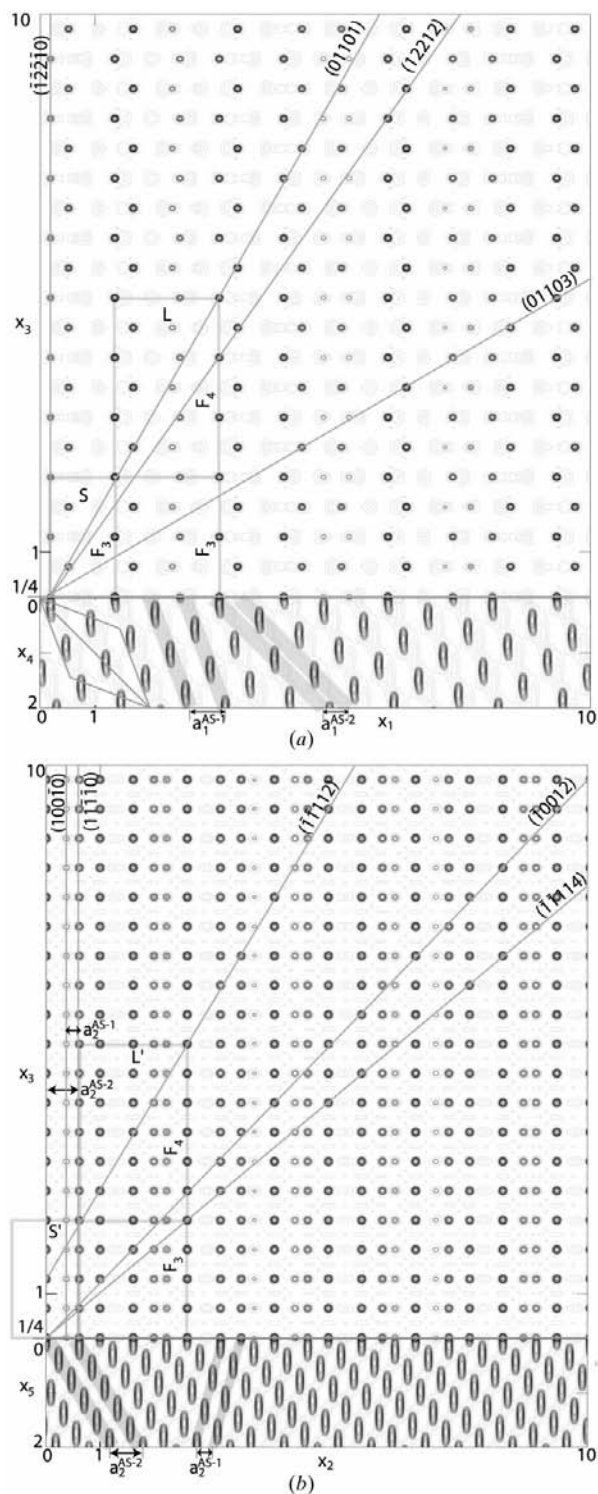


Figure 2
Structure of decagonal Al-Co-Ni (Cervellino *et al.*, 2001) projected onto (a) the (x_1, x_3) plane and (b) the (x_2, x_3) plane. The traces of net planes perpendicular to these planes are shown. The rectangles with edge lengths S and F_3 , and L and F_4 are the basic building units of this projection. In the lower part of the figures, the corresponding (x_1, x_4) and (x_2, x_5) plane, respectively, are depicted to illustrate the relationship between the parallel (x_1, x_2, x_3) and the perpendicular space (x_4, x_5) as well as the oblique projection directions to obtain average structures AS-1 and AS-2. The fundamental unit of size $L \times L' \times 3c$ contains just one stack of three large pentagonal prisms with TM at the corners ($d_{\text{TM-TM}} = 4.625 \text{ \AA}$).

respectively, corresponding to very strong Bragg reflections (Fig. 3). Their traces form angles $\Theta_{01101} = \arctan[\tau a_5 / (3 - \tau)^2 a_r] = 60.388 \dots$ and $\Theta_{11112} = \arctan[\tau a_5 / (3 - \tau)^{3/2} a_r] = 59.138 \dots^\circ$ with the positive x_1 and x_2 axes, respectively. Other net planes, similarly associated with strong Bragg reflections (*cf.* Table 1), can be found in the same way.

Thus, there exist not only inclined but at the same time periodically arranged net planes in DQC. Their structure can be understood and systematically described in terms of the ‘periodic average structure of quasicrystals’ (Steurer, 1999; Steurer & Haibach, 1999b; Steurer, 2001). It has been shown that all quasiperiodic structures fulfilling some conditions have periodic average structures. It is necessary that the quasiperiodic structures admit a finite-dimensional embedding superspace such that the actual structure may be thought of as an irrational section of a periodic hypercrystal in superspace. Furthermore, the structure needs to be described in perpendicular space by a finite density (we may think of it as a probability density), constant or smoothly varying, supported on appropriate finite convex polytopes (known as the *atomic surfaces*). It has been shown that convexity of the atomic surfaces is also a necessary and sufficient condition to have inflation symmetry (Masáková *et al.*, 1998, 2000; Berman & Moody, 1994),² which is another of the substantial features characterizing most known quasicrystals. Hence, by means of these two properties, we may distinguish neatly between (possibly disordered) on-average-ideal quasicrystals, having convex atomic surfaces and smooth probability density (probability values between 0 and 1 indicating structural disorder), and random tilings in their common ‘strong’ acceptance in which either the probability density is sharply varying on fractal atomic surfaces or, even more extremely, without any superspace embedding.

Employing the higher-dimensional approach, average structures can be obtained by oblique projection of the hypercrystal structure related to the quasicrystal (Figs. 2a and 2b). Appropriate projection directions, leading to different unit-cell dimensions of the average structure, depend on position and size of the atomic surfaces in the nD unit cell. Each atom of the quasiperiodic structure is assigned to one projected atomic surface of the average structure. However, depending on the type of oblique projection and shape of atomic surfaces, not every projected atomic surface of the average structure is assigned to exactly one atom of the quasiperiodic structure.

Based on the ‘periodic average structure’ approach, it is straightforward to find the net planes related to the densest atomic layers. These are simply the low-indexed lattice planes of the average structure itself. The atomic layers occupying

² The notion of convexity is a *geometric* one, hence it can be rigorously applied only to idealized atomic surfaces having constant probability density $\mathbf{P} = 1$. However, the concept can be easily extended to atomic surfaces having non-constant but smoothly varying probability density $\mathbf{P} \leq 1$. Given two points A, B of a given atomic surface [with $\mathbf{P}(A) > 0$ and $\mathbf{P}(B) > 0$] and any point C on the segment AB , we can define the atomic surface to be *statistically convex* if C belongs to the same atomic surface and $\mathbf{P}(C) > \min\{\mathbf{P}(A), \mathbf{P}(B)\}$.

Table 1

The 16 strongest reflections of decagonal Al₇₁Co₇Ni₂₂.

Listed are the 5D reflection indices $\mathbf{H} = (h_1h_2h_3h_4h_5)$, the corresponding indices on the reciprocal bases of four periodic average structures, the structure amplitudes $|F(\mathbf{H})|$, the net plane spacings $d_{\mathbf{H}}$ and the angles α between $[\mathbf{H}]$, the normals to the net planes, and the tenfold axis $[00001]$.

\mathbf{H}	$\mathbf{H}_{\text{AS-1}}$	$\mathbf{H}_{\text{AS-2}}$	$\mathbf{H}_{\text{AS-3}}$	$\mathbf{H}_{\text{AS-4}}$	$ F(\mathbf{H}) $	$d_{\mathbf{H}}$ (Å)	α (°)	Comments
00002	002	002	002	002	91.9	2.043	0	to base face
01101	101				69.4	2.019	60.4	to icosahedron edge
00004	004	004	004	004	54.4	1.021	0	to base face
11110	010				46.1	1.221	90	to lateral prism face
01103	103				46.1	1.175	30.4	to pentagon edge
11112	012				41.6	1.048	59.1	to decagon edge
10010		010			37.6	1.975	90	to observed lateral prism face
10012		012			34.5	1.420	46.0	to decagon edge
11110			100		28.8	3.757	90	to lateral prism face
13311				101	28.6	0.867	77.8	to lateral icosahedron face
11112			102		26.7	1.795	28.5	to pentagon edge
00006	006	006	006	006	25.6	0.681	0	to base face
12212		102			24.9	1.174	54.9	to pentagon edge
21120			010		24.5	0.754	90	to lateral prism face
12210		100			24.5	1.435	90	to lateral prism face
11114	014				24.2	0.783	39.9	to decagon edge

these planes are not perfectly flat. Their corrugation, *i.e.* the maximum distance of the atoms to the respective plane, is determined by the dimensions of the projected atomic surfaces. We will in the following consider two important average structures between the many possible ones. The first periodic average structure (AS-1) is obtained by the kernel (01010) for the oblique projection upon the (x_1, x_3) plane, and by the kernel (11011) for the oblique projection upon the (x_2, x_3) plane. This leads to the average structures with lattice parameters $a_1^{\text{AS-1}} = 5a_r/(2\tau^2) = (3 - \tau)^2 a_r/2 = 2.322$ and $a_2^{\text{AS-1}} = (3 - \tau)^{3/2} a_r/(2\tau) = 1.221$ Å (Fig. 4).

Under certain conditions, the decagonal phase transforms into the β phase (*cf.* the discussion in Steurer, 1999, and references therein).³ The geometrical relationships between these two phases becomes clear when another average structure (AS-2) is used with lattice parameters $a_1^{\text{AS-2}} = 5a_r/\tau^3 = (3 - \tau)^2 a_r/\tau = 2.870$, $a_2^{\text{AS-2}} = 5a_r/[(3 - \tau)^{1/2} \tau^2] = a_r(3 - \tau)^{3/2} = 3.950$ Å. One sees easily that the net planes of the DQC and the β phase are parallel (Figs. 4*b* and 4*d*). Much more, the average structure AS-2 of the DQC coincides with the CsCl-type structure of the β phase itself.

2.2. Structure of net planes

In the case that a net plane contains all atoms of the quasiperiodic layers within one translation period, there must be a one-to-one relationship between the atoms of the layers and the atoms of the net plane. If the corrugation of the inclined atomic layers is neglected, the structure of the net plane then corresponds just to a projection along x_3 of the quasiperiodic atomic layers in $x_3 = 1/4$ and $x_3 = 3/4$ upon the net plane. This is illustrated in Fig. 5(*a*) for the net plane (01101). The pentagonal structure motifs formed by transition

³ Particularly interesting for the relation with the DQC growth mechanism is the fact that the β phase has also been found as phase transformation product on the surface of DQC (Zurkirch *et al.*, 1998; Shimoda *et al.*, 2000, and references therein).

metals (TM), with edge length $a_r\tau(3 - \tau)^{1/2} = 4.625$ Å, are drawn in the atomic layer at $x_3 = 1/4$ (Fig. 5*b*). The same TM pentagon is seen distorted in the net plane (01101) owing to the oblique projection upon it (Fig. 5*a*). The face form {01101} describes the pyramid faces of the unit polyhedron, a pentagonal bipyramid with the TM pentagon as base and of total height $3c$. This unit polyhedron is also found in the approximants of decagonal Al-Co-Ni (*cf.* Steurer, 2000).

The TM pentagon is also the smallest structural feature that can be considered ideally inflation-invariant⁴ on scaling (upwards) by integral powers of τ . The values of the lengths shown in Fig. 5 are, respectively, $S = a_r\tau^2(3 - \tau)/2$, $L = \tau S = a_r\tau^3(3 - \tau)/2$, $S' = a_r\tau(3 - \tau)^{1/2}$, $L' = \tau S' = a_r\tau^2(3 - \tau)^{1/2}$. The values of L and L' correspond just to the dimensions of a projected large pentagon (Fig. 5*b*) upon the (x_1, x_3) and the (x_2, x_3) planes, respectively. We will see how the average structures and the net planes are strictly related to these important structural features.

Figs. 2(*a*) and 2(*b*) show that the projected structure can be broken down into rectangular unit cells with widths S, S', L, L' , and heights F_3c, F_4c . F_3, F_4 are Fibonacci numbers, defined recursively by $F_0 = 0, F_1 = 1, F_{n+1} = F_n + F_{n-1}$. The trace of the net plane (01101) inside these rectangles in the (x_1, x_3) plane is very close to the respective diagonal vectors $\mathbf{s}_1 = (S, F_3c) = (a_r\tau^2(3 - \tau)/2, 2c)$ and $\mathbf{l}_1 = (L, F_4c) = (a_r\tau^3(3 - \tau)/2, 3c)$. The trace of the net plane (11112) in the (x_2, x_3) plane is correspondingly close to $\mathbf{s}_2 = (S', F_3c) =$

⁴ This is related to the fact that a Penrose tiling of edge $\tau^3 a_r$ has been found (Cervellino *et al.*, 1998) to have structural relevance, in the sense that (*a*) on such a scale a tiling can ideally represent the DQC but not at a lower scale (particularly at the bond-length scale, with tile edge a_r) because of structural disorder; (*b*) accordingly, inflation symmetry is ideally fulfilled from this scale up. Accordingly, the named pentagon is the τ^3 -inflated version of the smallest coordination polygon induced by this crystal's atomic surfaces. As it has edge length 0.928 Å, only one vertex of this minimal pentagon can be occupied ($\mathbf{P} < 1/5$), while the τ^3 -inflated pentagon is fully occupied ($\mathbf{P} = 1$). It is not surprising that the generalized $(x_i, x_j)_{i=1,2}$ inflation operation $\tilde{\tau}^n$ (see text) will force the same 'natural' minimal scale.

$(a_r\tau(3 - \tau)^{1/2}, 2c)$ and $I_2 = (L', F_4c) = (a_r\tau^2(3 - \tau)^{1/2}, 3c)$. Its maximum distance is given by the boundaries of the projected atomic surfaces of the average structure of the quasiperiodic structure. This is the consequence of the following correspondence principle: if the quasiperiodic structure and its average structure are superposed then all vertices of the quasiperiodic structure fall inside the projected atomic surfaces of the average structure. If the vertices of the quasiperiodic structure are now decorated with the projected atomic surfaces of the average structure then all lattice nodes

of the average structure fall inside the now quasiperiodically distributed projected atomic surfaces.

Consequently, the τ^n scaling operation can be extended to the $(x_i, x_3)_{i=1,2}$ planes. The (x_1, x_2) -projected structures are known to be invariant under τ^n scaling; the x_3 direction is periodic in c and this excludes irrational scaling. However, scaling by integer numbers is allowed and the Fibonacci numbers are integers. Their remarkable properties $\lim_{n \rightarrow \infty} F_n/F_{n-1} = \tau$ and $\tau^n = F_n\tau + F_{n-1}$ allow us to redefine the τ^n scaling operation $\hat{\tau}^n$ as $\hat{\tau}^n : (x, zF_m c) \rightarrow (x\tau^n, zF_{n+m}c)$.

Consider now scaled sequences of vectors ($n = 0, 1, \dots$): $\mathbf{v}_n(x, z, m) = \hat{\tau}^n v(x, z, m) = \hat{\tau}^n(x, zF_m c) = (x\tau^n, zF_{n+m}c)$. Put $x = S, z = 1, m = 3$ and the first two terms of the sequence will be \mathbf{s}_1 and I_1 . In the same way, with $x = S', z = 1, m = 3$, we obtain a sequence having \mathbf{s}_2 and I_2 as the leading terms. Consider now the associated sequence of angles $\varphi_n(x, z, m) = \arctan(zF_{n+m}c/x\tau^n)$. Owing to the properties of the Fibonacci numbers and the numeric relations $\tau^2 = \tau + 1$ and $5 = (3 - \tau)^2\tau^2$, we can write:

$$\begin{aligned} \Phi(x, z, m) &= \lim_{n \rightarrow \infty} \varphi_n(x, z, m) \\ &= \lim_{n \rightarrow \infty} \arctan\{za_5/[x\tau^{-n}(\tau + F_{n+m-1}/F_{n+m})]\} \\ &= \arctan\{za_5/[x\tau^{-n}(\tau + 1/\tau)]\} \\ &= \arctan\{za_5/[x\tau^{1-n}(3 - \tau)]\}. \end{aligned}$$

So, $\Phi(S, 1, 3) = \arctan\{c/[S\tau^{-2}(3 - \tau)]\} = \arctan(c/a_1^{AS-1})$, and, similarly, $\Phi(S', 1, 3) = \arctan[(c/2)/a_2^{AS-1}]$. The $n \rightarrow \infty$ limit slopes of the \mathbf{v}_n vectors coincide visibly with the $\{101\}$ and $\{021\}$ lattice planes of AS-1. Moreover, it is easy to see that $\Phi(S, 1, 3) = \Theta_{01101}$ and $\Phi(S', 1, 3) = \Theta_{\bar{1}\bar{1}112}$, so the limit slopes coincide with the considered DQC net planes. As a consequence of inflation symmetry, every vector⁵ \mathbf{v}_n is an interatomic vector because the leading terms are so. This allows one to determine the relation of atoms belonging to any given structure motif with the DQC net planes.

It is clear that mathematically flat atomic layers are not possible in a DQC in directions other than parallel or perpendicular to the quasiperiodic layers. This is a consequence of the fact that the projected atomic surfaces of the average structure are not point-like but extended objects. The considered net planes must necessarily be corrugated. The \mathbf{v}_n vector sequences allow the determination of the maximal corrugation. Set the origin of the \mathbf{v}_n vectors on an atom lying on the trace of the corresponding net planes. The \mathbf{v}_n vector tips will be on atoms belonging to the same (inflated) structure motif. We can calculate the distance d_n of these atoms from the net plane trace. It is $d_n = \|\mathbf{v}_n\| |\sin(\varphi_n - \Phi)|$; clearly, $\|\mathbf{v}_n\|$ goes as τ^n for $n \rightarrow \infty$. We will show that $|\sin(\varphi_n - \Phi)|$ goes as $(1/\tau)^{2n}$ for $n \rightarrow \infty$, so that d_n goes as $(1/\tau)^n$. In fact, putting $\tan(\varphi_n) = (1 + \varepsilon_n)\tan(\Phi)$, to the first order in ε_n , we have $\sin(\varphi_n - \Phi) \cong \varepsilon_n \sin(2\Phi)/2$. Substituting the expressions given above for Φ and φ_n and using the aforesaid properties of F_n and τ , we have

⁵ For notational conciseness, we will drop in the following the functional dependence from (x, z, m) . Notice that the \mathbf{v}_n vector sequences have a 'natural' minimal scale ($m = 3$, cf. footnote 4).

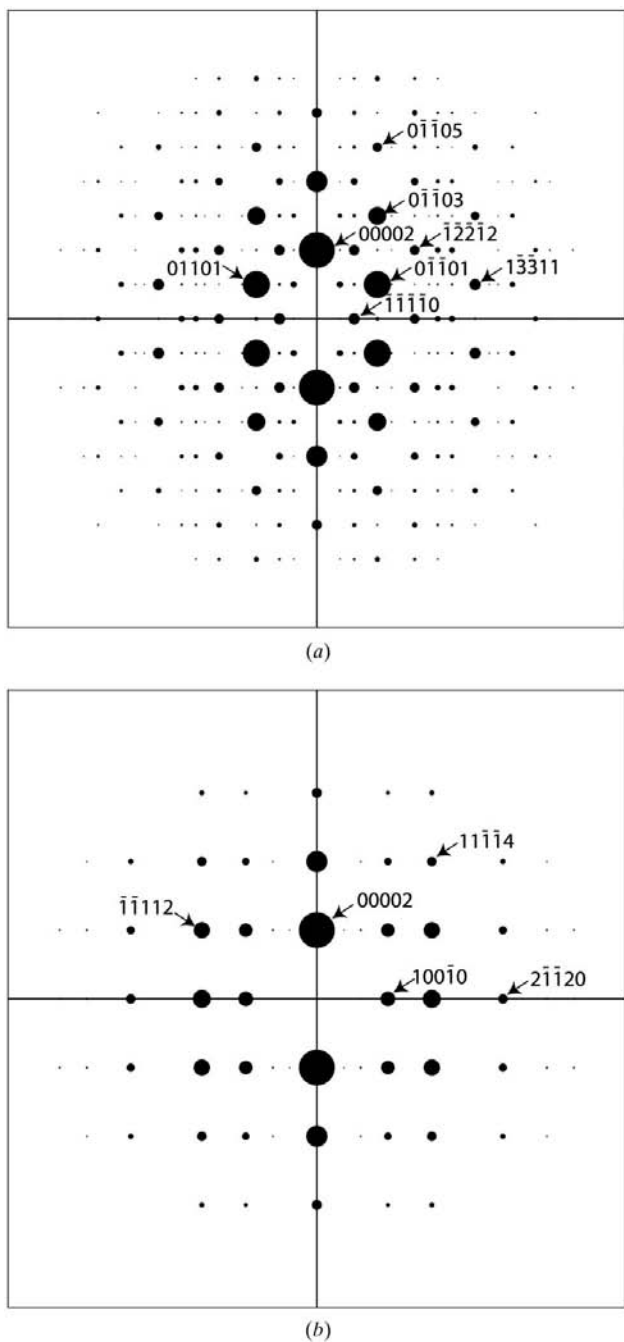


Figure 3
(a), (b) Reciprocal-space sections of decagonal Al-Co-Ni (Cervellino *et al.*, 2001) corresponding to the structure projections on the (x_1, x_3) and (x_2, x_3) planes (Fig. 2), respectively. The size of a dot is proportional to the experimentally observed intensity of the reflection it marks.

$$\begin{aligned}
 \varepsilon_n &= [(3 - \tau)\tau F_{n+m} - \tau^{n+m}]/(\tau^{n+m}) \\
 &= [(2\tau - 1)F_{n+m} - \tau^{n+m}]/(\tau^{n+m}) \\
 &= (\tau F_{n+m} - F_{n+m} - F_{n+m-1})/(\tau^{n+m}) \\
 &= -[(-1/\tau)F_{n+m} + F_{n+m-1}]/(\tau^{n+m}) \\
 &= (-1)^{n+m}(1/\tau)^{2(n+m)}.
 \end{aligned}$$

Here we used also the derived properties $1/\tau = \tau - 1$ and $(-1/\tau)^n = F_n(-1/\tau) + F_{n-1}$ (this is because $-1/\tau$ is the conjugate of τ as a Pisot number). As a result, the atoms on

the tips of the \mathbf{v}_n vectors will come exponentially closer to the net plane as $n \rightarrow \infty$. The largest deviations from the planes occur for $n = 1$; for both the (01101) and ($\bar{1}\bar{1}112$) planes, this is smaller than 0.14 Å.

2.3. Inclined net planes and growth of DQC

The equilibrium morphology of crystals can be understood and predicted from the knowledge of the atomic planes with the lowest specific surface energy. These atomic planes

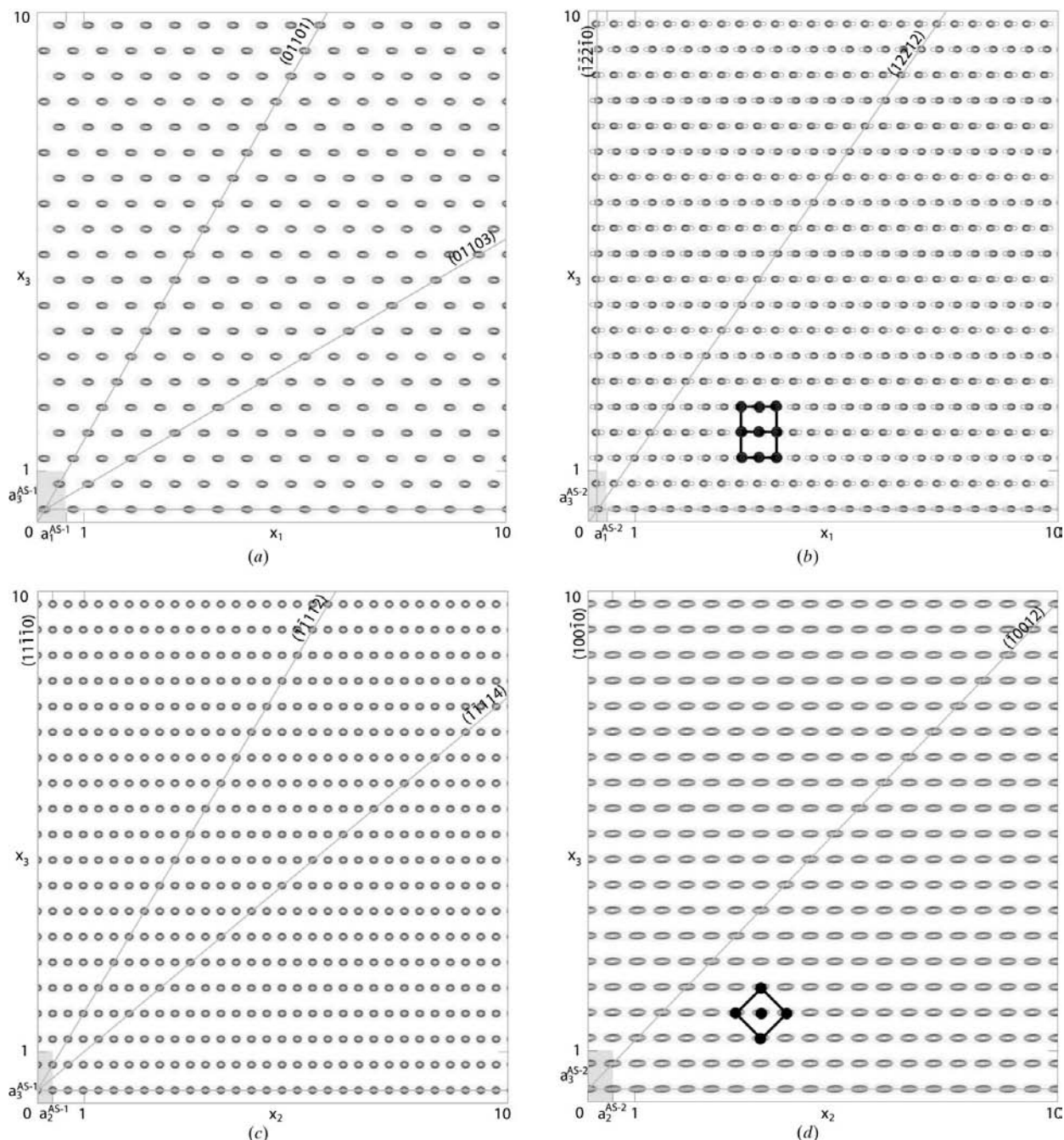


Figure 4 Average structures of decagonal Al-Co-Ni (Cervellino *et al.*, 2001) projected onto (a), (b) the (x_1, x_3) plane and (c), (d) the (x_2, x_3) plane. The average structures AS-1 and AS-2 are shown in (a), (c) and (b), (d), respectively. The traces of net planes perpendicular to these planes are shown.

correspond to dense net planes containing important *periodic bond chains* (PBC) according to the PBC theory (*cf.* Hartman, 1987, and references therein). PBC are uninterrupted chains of strong atomic bonds. To understand the morphology of quasicrystals, the PBC theory can be applied in a modified form – *quasiperiodic bond chains* (QBC) instead of periodic bond chains have to be considered. This has been performed to some extent by Ho *et al.* (1987) who developed a theory of faceting in bond-oriented glasses and icosahedral quasicrystals based on *perfect bond-oriented systems* (PBOS), by Janssen *et al.* (1989), who discussed how to characterize the

morphological importance of crystal growth faces, by Kremers *et al.* (1995), Heijmen *et al.* (1995) and van Smaalen (1993, 1999), who studied the morphology of all kinds of aperiodic crystals. Toner (1990) studied theoretically growth and kinetic roughening of icosahedral quasicrystals, *i.e.* their non-equilibrium growth morphology. According to Liu *et al.* (2000), the growth mechanism of DQC should be similar to that of regular crystals along the periodic direction and similar to that of icosahedral phases in the quasiperiodic plane. They found a roughening transition temperature where the lateral growth mode changed into a continuous growth mode, and the growth pattern changed from a faceted to an equiaxial structure.

Employment of the modified PBC theory makes it easy to find the most probable face form describing the decaprisms faces. The strongest Bragg reflections indicate $\{100\bar{1}0\}$ or $\{11\bar{1}\bar{1}0\}$ and $\{\bar{1}\bar{1}\bar{1}10\}$ as most probable candidates. The planes $(100\bar{1}0)$ and $(11\bar{1}\bar{1}0)$ perpendicular to x_2 and $(\bar{1}\bar{1}\bar{1}10)$ perpendicular to x_1 . Since the shortest bonds of length $a_r = 2.432 \text{ \AA}$ within the quasiperiodic layers, and also those linking neighbouring quasiperiodic layers (2.518 \AA) are parallel to the (x_1, x_3) plane, the strongest PBC are parallel to $\{100\bar{1}0\}$ and $\{11\bar{1}\bar{1}0\}$. This agrees with the experimental observations.

Since inclined net planes are never perfectly flat, the adding of atoms during the growth process is energetically favourable compared with starting a new net plane on a flat surface. Consequently, owing to their high growth rate, these facets can only be observed on very tiny non-equilibrium crystals. It is remarkable, however, that the base face (00001) and the facets inclined to $[00001]$ are of comparable size in Fig. 1. Thus, the specific surface energies of these faces seem to be of the same order of magnitude. Any perturbation or termination of a net plane containing PBC increases its energy. Therefore, the energy should show a minimum for a system with the maximum number of undisturbed net planes. In the case of bipyramidal face forms of the type $\{h_1h_2h_3h_4h_5\}$ with $h_5 \neq 0$, this is only possible for quasiperiodically ordered structures without any stacking faults along the periodic direction. Indeed, no disorder in the periodic stacking of quasiperiodic layers (in diffraction patterns indicated by diffuse streaking parallel to the tenfold axis) has ever been observed in stable DQC. Much more, even the existence of only two sets of inclined net planes being orthogonal to each other is sufficient to force quasiperiodicity due to the scaling symmetry discussed above.

Each of the two sets of periodic net plane stacks, (01101) and $(\bar{1}\bar{1}112)$, contains all atoms of the DQC. We can generate the vector sequences \mathbf{v}_n by applying the Fibonacci substitution rule ($\mathbf{s}_i \rightarrow \mathbf{I}_i, \mathbf{I}_i \rightarrow \mathbf{I}_i\mathbf{s}_i$) starting from the appropriate leading terms. This substitution rule corresponds to ideal quasiperiodic long-range order. If we consider only one set of net planes, then any ordering of \mathbf{s}_i and \mathbf{I}_i units would be acceptable because the deviations would anyway remain small. Considering both sets of planes and all symmetrically equivalent sets too, only quasiperiodic ordering is compatible with a maximally flat net plane ensemble. This can be easily understood in terms of the average structure approach. Any deviation from

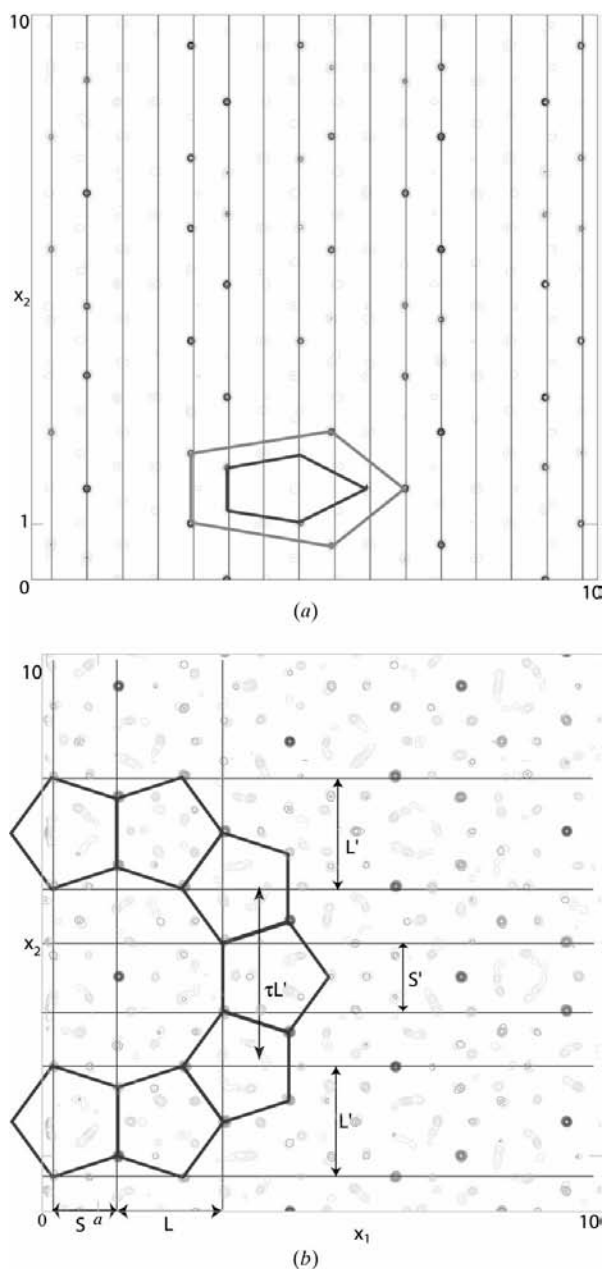


Figure 5
(a) Structure of the net plane $(01\bar{1}01)$. (b) Quasiperiodic atomic layer of decagonal Al–Co–Ni with $x_3 = 1/4$ (Cervellino *et al.*, 2001). Some geometrical structure motifs and unit lengths are marked.

quasiperiodicity increases the size of the atomic surfaces and therewith also the size of its projected images. Strongly overlapping projected atomic surfaces lead to a more or less continuous probability density distribution in the average structure and the concept of net planes loses its meaning.

3. Conclusions

In a strict sense, there are no net planes in DQC inclined to the tenfold axis but the net planes of their periodic average structures. This has the consequence that atomic layers inclined to the tenfold axis are always slightly puckered. Since inclined net planes link periodic with quasiperiodic directions in decagonal quasicrystals, they may play a crucial role in establishing quasiperiodic long-range order. Any randomness destroys locally the planarity of net planes. A random tiling-based quasicrystal would not show any net planes at all.

WS wants to thank Dr J. Schreuer for useful discussions. Financial support by the Swiss National Science Foundation, contract No. 20-53630.98, is gratefully acknowledged.

References

- Ashcroft, N. W. & Mermin, N. D. (1976). *Solid State Physics*, pp. 151–162. Philadelphia: Saunders College.
- Berman, S. & Moody, R. V. (1994). *J. Phys. A: Math. Gen.* **27**, 115–130.
- Boudard, M., de Boissieu, M., Janot, C., Heger, G., Beeli, C., Nissen, H. U., Vincent, H., Ibberson, R., Audier, M. & Dubois, J. H. (1992). *J. Phys. Condens. Matter*, **4**, 10149–10168.
- Cervellino, A., Haibach, T. & Steurer, W. (1998). *Phys. Rev. B*, **57**, 11223–11231.
- Cervellino, A., Haibach, T. & Steurer, W. (2001). In preparation.
- Donnay, J. D. H. & Harker, D. (1937). *Am. Mineral.* **22**, 446–467.
- Hartman, P. (1987). *Morphology of Crystals*, edited by I. Sunagawa, pp. 269–319. Tokyo: Terra Scientific Publishing Company.
- Heijmen, T. G. A., Kremers, M. & Meekes, H. (1995). *Philos. Mag.* **B71**, 1083–1100.
- Ho, T. L., Jaszczak, J. A., Li, Y. H. & Saam, W. F. (1987). *Phys. Rev. Lett.* **59**, 1116–1119.
- Huang, X. & Gong, C. (1998). *Phys. Rev. B*, **58**, 739–744.
- Janssen, T., Janner, A. & Bennema, P. (1989). *Philos. Mag.* **B59**, 233–242.
- Jaszczak, J. A. (1994). *Mineral. Record*, **25**, 85–93.
- Kremers, M., Meekes, H., Bennema, P., Verheijen, M. A. & Vandereerden, J. P. (1995). *Acta Cryst.* **A51**, 716–739.
- Levine, D. & Steinhardt, P. J. (1986). *Phys. Rev. B*, **34**, 596–616.
- Liu, Y. C., Yang, J. H., Guo, X. F., Yang, G. C., Zhou, Y. H. & Zhu, R. H. (2000). *Mater. Lett.* **43**, 320–323.
- Masáková, Z., Patera, J. & Pelantová, E. (1998). *J. Phys. A: Math. Gen.* **31**, 4927–4946.
- Masáková, Z., Pelantová, E. & Svobodová, M. (2000). *Lett. Math. Phys.* Submitted.
- Shimoda, M., Guo, J. Q., Sato, T. J. & Tsai, A. P. (2000). *Surf. Sci.* **454–456**, 11–15.
- Smaalen, S. van (1993). *Phys. Rev. Lett.* **70**, 2419–2422.
- Smaalen, S. van (1999). *Acta Cryst.* **A55**, 401–412.
- Socular, J. E. S. & Steinhardt, P. J. (1986). *Phys. Rev. B*, **34**, 617–647.
- Steurer, W. (1999). In *Proceedings of the International Conference on Solid-Solid Phase Transformations '99*, edited by M. Koiwa, K. Otsuka & T. Miyazaki, pp. 1333–1336. Tokyo: The Japanese Institute of Metals.
- Steurer, W. (2000). *Z. Kristallogr.* **215**, 323–334.
- Steurer, W. (2001). *Ferroelectrics*. In the press.
- Steurer, W. & Haibach, T. (1999a). *Physical Properties of Quasicrystals*, edited by Z. Stadnik, pp. 51–89. Heidelberg/New York: Springer.
- Steurer, W. & Haibach, T. (1999b). *Acta Cryst.* **A55**, 48–57.
- Toner, J. (1990). *Phys. Rev. Lett.* **64**, 930–933.
- Zurkirch, M., Bolliger, B., Erbudak, M. & Kortan, A. R. (1998). *Phys. Rev. B*, **58**, 14113–14116.